Subwavelength colour imaging with a metallic nanolens

SATOSHI KAWATA[1,2]*, ATSUSHI ONO[2] AND PRABHAT VERMA[1,3]

[1]Department of Applied Physics, Osaka University, Suita, Osaka 565-0871, Japan
[2]Nanophotonics Laboratory, RIKEN, Wako, Saitama 351-0198, Japan
[3]Department of Frontier Biosciences, Osaka University, Suita, Osaka 565-0871, Japan
*e-mail: kawata@skawata.com

Published online: 15 June 2008; doi:10.1038/nphoton.2008.103

Early research into metamaterials by other scientists has shown that nanostructured metamaterials can focus incident light and act as a lens. Although such structures are capable of subwavelength imaging, they have two major restrictions: they can only work at one particular wavelength, and the image can only be transferred for a short distance within the limits of the near field and is therefore undetectable in the far field. Here, we propose a lens made of stacked silver nanorods that is capable of colour imaging at subwavelength resolution in the visible range. The subwavelength image can be transferred over distances of at least micrometre scale and magnified before detection by conventional optics devices. Such a nanorod lens has the potential to be an indispensable imaging tool, with particular application to biomedical applications, where individual viruses and other nano-entities could be imaged in colour in the far field.

Metamaterials have received a great deal of attention in the recent past, because such materials can be artificially engineered to cause negative refraction (negative permittivity together with negative permeability), resulting in subwavelength image formation[1–8]. Subwavelength resolution can be achieved only when the fast-decaying evanescent component of the radiation is involved in the process of image formation. If electromagnetic energy is transferred through plasmons, it is possible to maintain the evanescent component in the process of image formation. In extreme near-field conditions (such as very close to a metallic structure), the electric and magnetic fields of electromagnetic radiation become almost independent of one another. For example, for *p*-polarization of the evanescent component, the magnetic field can be neglected, and only the permittivity of the material is of importance. Therefore, some common metals can work, to a good approximation, as metamaterials under an extreme near-field configuration. Silver serves as a good metamaterial under such conditions, which has recently led several groups to demonstrate the transfer of electromagnetic energy back and forth through the surface plasmons of silver nanostructures. The research groups of Pendry[1,2], Smith[3] and Zhang[6] have discussed plasmon propagation in bulk metamaterials, and Atwater and colleagues have demonstrated[9,10] a waveguide-like transfer of plasmon energy through a chain of metallic nanoparticles. Fabrication of metamaterials is also a big issue, and several other groups have been involved in fabrication techniques[11–14] that can potentially help in engineering metamaterials for practical demonstrations.

It has been predicted[1] that there will be amplification of the evanescent component of the radiation in a silver slab through the resonant interaction of the component with surface plasmons propagating parallel to the surface of the slab (perpendicular to the radiation). In our earlier report[7], we predicted the transfer of near-field energy through silver nanorods, where the radiation energy coupled resonantly with plasmons propagating parallel to the radiation, to result in extreme subwavelength imaging. The predominant shortcoming of these and other similar reports is that they deal only with one particular wavelength, leaving a major restriction that only objects emitting a particular wavelength can be imaged. Another shortcoming is that there is usually no way to detect these subwavelength images at the far field or to record them using diffraction-limited optics. There are a few recent reports demonstrating the magnification of subwavelength images[15–17]; however, these deal with single wavelength imaging. A colour object, in these cases, would not make a sharp image, and long-distance image transfer would be impossible due to the dispersion of plasmon energy in the imaging process. The metallic nanolens we propose here, in contrast, can transfer colour images at subwavelength resolution through stacked layers of silver nanorod arrays, which can be detected in the far field owing to the magnification of the image. Because the transfer of energy in our design occurs by means of the resonant modes of plasmons travelling parallel to the radiation, we have sufficient enhancement to ensure a long-distance image transfer without significant dispersion of energy. Figure 1a presents a schematic of a metallic nanolens arrangement, in which magnified long-distance colour imaging is described.

RESULTS

LONG-DISTANCE IMAGE TRANSFER

In order to realize a long-distance subwavelength image transfer, let us first consider imaging through a 50-nm-long silver rod with a diameter of 20 nm and establish the effect of increasing the rod length. The transfer of the near-field energy occurs through the resonance modes of a plasmon propagating along the length of an individual nanorod (Fig. 1b). The field enhancement is

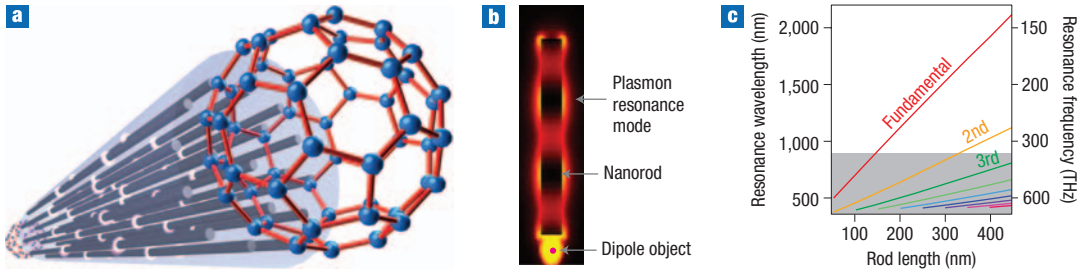

Figure 1 Optical energy transfers plasmonically through the lengths of silver nanorods. a, Illustration of long-distance image transfer through a metallic nanolens that provides a magnified colour image with subwavelength spatial resolution. **b**, Simulation results for plasmon resonance modes propagating along the length of a silver nanorod. A dipole object is set near one end of the rod, and the light energy travels through the resonating plasmon modes to the other end of the rod. **c**, Plot showing that the frequency positions of plasmon resonance modes depend strongly on the length of the rod.

typically of the order of between $\sim 1 \times 10^5$ and $\sim 1 \times 10^6$, which ensures sufficient intensity at the image plane. The resonance wavelengths, as well as the number of modes, depend strongly on the length of the nanorod. The effect of increasing rod length can be seen in Fig. 1c, which shows that the resonance wavelengths shift to the red, and higher-order modes start appearing with increasing rod length. The fundamental mode of resonance jumps out of the visible range (shown by the grey area in Fig. 1c) with increasing rod length, which makes it impossible to transfer an image of an object emitting visible light over a long distance.

In order to overcome this problem, we propose a stacked arrangement of nanorod arrays, which is capable of transferring the image of a visible object over a much longer distance. We explain the concept of the proposed nanolens with an example of a stacked arrangement of three layers of nanorod arrays, separated by 10 nm, each containing 50-nm-long rods, each with a diameter of 20 nm (Fig. 2a). The image of the letter 'A' in Fig. 2a was calculated using a three-dimensional finite-difference time-domain (3D-FDTD) method by taking account of the complex dielectric function of silver[18]. The blurring of pixels in the image is accounted for by the point spread function in the imaging process. The nanorods are arranged at a pitch of 40 nm, which dictates the imaging resolution and also guarantees no crosstalk between neighbouring rods[7]. In this new arrangement, the object source excites the resonance modes of local plasmons in the rods of the first layer, which couple with the resonance modes of local plasmons in the rods of the second layer at the nanogap between the two layers, and then to the third layer in the same fashion, to finally provide an image at the other end of the third layer. Although the image transfer in this case is over a total length of 170 nm (three 50-nm rods + two 10-nm gaps), the local plasmons are excited in each layer individually, through their couplings at the gaps. Therefore, one would expect the effective resonance response to be closer to that of a 50-nm rod, rather than that of the total length of the nanolens. Indeed, we found this prediction to be correct in our simulation results, which showed that the plasmon resonance for the strongest mode of the stacked arrangement was at 622 THz, which is the same as the frequency of the fundamental mode of a 50-nm-long nanorod. We found similar results when the number of layers was further increased. This confirms that we can overcome the situation predicted in Fig. 1c, as the effective plasmon resonance stays in the visible region even if the total length of image transfer is increased remarkably, making it possible to have a long-distance image transfer in the visible range.

In order to confirm the long-distance transfer of an image without suffering significant loss, we simulated the transfer of light energy for an increasing number of layers. Figure 2b presents a comparison of simulation results for the intensity distribution along the length of the nanolens for three cases, in which the nanolens comprises 3, 9 and 17 layers of nanorod arrays. In each case, the unit rod length is 50 nm, and the gap between the layers is 10 nm. The nanolens comprising 17 layers has a total length of over 1 μm. The upper, coloured images in Fig. 2b show a cross-sectional view of the intensity distribution along the length of the nanolenses. The dotted rectangles within the image define the individual nanorods. The green, blue and red curves indicate the line profiles of the intensity distribution along the axes of the nanolenses having 3, 9 and 17 layers, respectively. The vertical dotted line coinciding with the strongest peaks at the left end of each curve indicates the position of the object (a point source). The y axis represents the intensity and the x axis represents the length of the nanolens. The zero of the x axis coincides with the entrance position of the nanolens, and the three vertical dotted lines mark the exit positions of the indicated nanolenses. A comparison between the three curves reveals that the intensity profiles have no noticeable dependence on the number of layers. The horizontal dotted line, which is a guide to the eye, indicates that the intensities at the exits of the three nanolenses are almost the same. It also indicates that there is no downward trend of the intensity line profile with increasing length of the nanolens, confirming that there is no significant loss of energy along the length of the nanolens. The linewidth of the point spread function at the exit of 17 layers, shown in the inset of Fig. 2b, is 30 nm, which is the same as that for a single layer. This essentially means that there is no recognizable blurring of the image, even after a distance of 1 μm. Furthermore, because the energy is transferred across the nanolens through the resonance modes of local plasmons and their interactions at the gap through the evanescent field, there are no long propagations of either plasmons or electromagnetic field in the process of image formation, which minimizes the propagation- and radiation-related losses. Our simulations thus confirm image transfer without significant loss over micrometre-scale distances. Because of computational limitations, we simulated a device with only up to 17 layers (equivalent to a total length of 1 μm); however, this is not the limit for efficient image formation. It is definitely possible to have more than 17 layers, and a similar evolution of the intensity distribution would still be expected along the nanolens over longer distances.

BROADBAND RESONANCE FOR COLOUR IMAGING

The other important feature of stacked arrangement of nanorods is colour imaging. Colour imaging requires the resonance to be

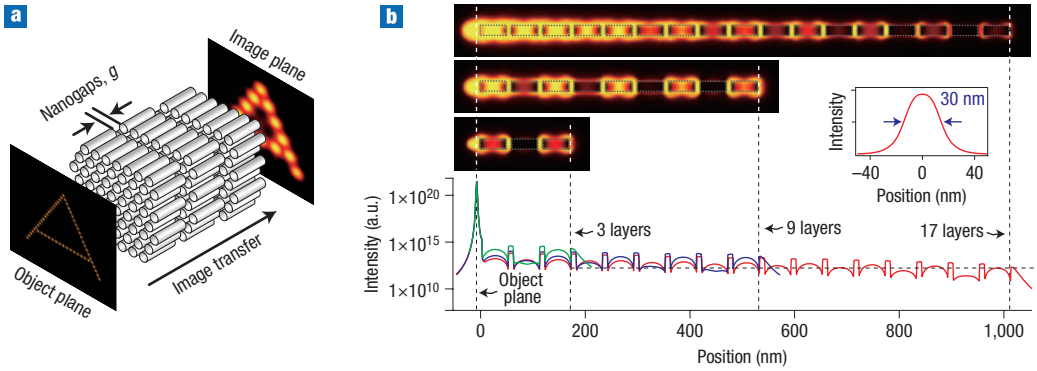

Figure 2 Long-distance image transfer can be realized through a stacked arrangement of nanorod arrays. a, The basic concept of the stacked arrangement of nanorod arrays for long-distance image transfer. In this example, a three-layered stacked arrangement is presented. The image of the letter 'A' is obtained from simulations based on 3D-FDTD calculations. **b**, Intensity profiles across 3-, 9-, and 17-layered stacked arrays, showing that neither intensity nor the point spread function has any noticeable dependence on distance, at least up to micrometre-scale distances. The inset shows the linewidth of the point spread function at the exit of 17 layers.

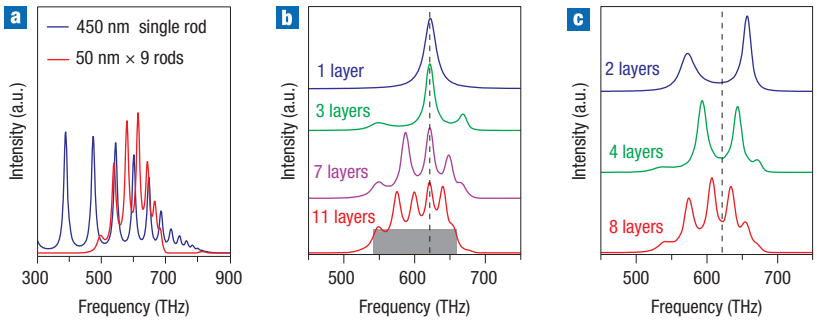

Figure 3 The resonance band becomes broader with an increasing number of layers. a, Comparison of the spread of the resonance modes for a divided rod (red curve) and a corresponding undivided rod (blue curve). **b**, For an arrangement with an odd number of layers, the number of resonance modes increases with the number of layers, and they collect around the fundamental mode of the corresponding unit rod to form a wide resonance band. **c**, For an arrangement with an even number of layers, the resonance modes have a similar feature of broadening, but there is no resonance mode at the frequency of the fundamental mode for the corresponding unit rod.

broad, so that a large part of the visible spectrum can be covered. Simulation results show that with an increasing number of layers, the number of resonant modes also increases, and they tend to gather in the vicinity of the fundamental mode of the corresponding unit rod. Figure 3a shows a comparison of the spread of resonance modes for a single 450-nm-long rod (blue curve) and such a rod divided into nine segments (50 nm each) separated by gaps of 10 nm (red curve). Although the resonance modes for the single rod are discretely spread out, the resonance modes of the divided rod tend to merge into a wide band in the visible range, ensuring a wide band resonance. Interestingly, when we consider the effect of increasing the number of layers, we find that the strongest mode always coincides with the fundamental mode of the unit rod, and all other modes tend to collect in the vicinity of the same. As can be seen from Fig. 3b, increasing the number of layers results in a broad resonance spread around the fundamental of the unit rod. For the arrangement having 11 layers, a large range of the visible frequency (from ~540 to ~670 THz) resonates with sufficient bias (intensity is non-zero and sufficiently high for observation; shown by the grey area). The bias increases with an increasing number of layers, ensuring flatter resonance throughout the resonance band. This broadening in the resonance band arises owing to the interaction of the local plasmons of individual unit rods at the gaps between them. The interaction perturbs the resonance frequencies of the plasmon modes, and the discrete modes turn into broad bands. The mechanism is analogous to the broadening process of the electronic energy band of an assembly of atoms in comparison with the energy levels of an isolated atom. This broadening of the resonance band is very useful for colour imaging, because with a large number of layers a broad spread of visible light would resonate and contribute to the imaging process. However, it should be noted here that for an even number of layers, the plasmon mode coinciding with the frequency of the fundamental for the corresponding unit rod is in a destructive condition (destructive interference of energy at 622 THz, as seen in Fig. 3c, and thus intensity at the frequency corresponding to the fundamental mode of a unit rod is very weak), so there is no resonance mode at this frequency. Figure 3c shows resonance modes for some arrangements with an even number of layers, where the resonance mode at 622 THz (the frequency of the fundamental mode for a 50-nm rod) is missing in every case. The results tell us that for a successful long-distance image transfer, a stacked arrangement with an odd number of layers is required.

GAP SIZE DEPENDENCE

The primary difference between the blue and red curves in Fig. 3a is the gap size, because the former can be considered as a special case

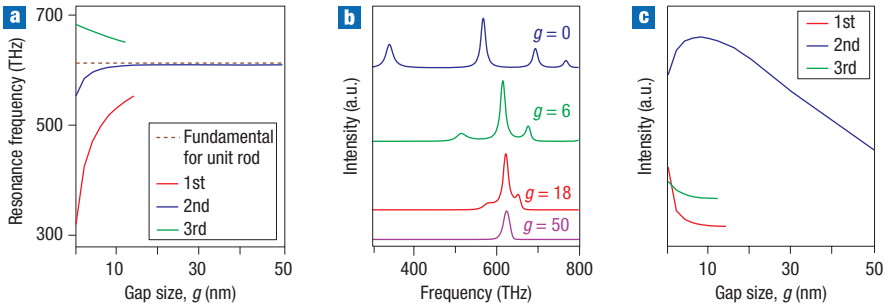

Figure 4 Gap-size dependence for the stacked layers of metallic nanorods. a, The gap dependence of the resonance modes for a 150-nm rod divided into three 50-nm-long rods. With increasing gaps between the rods, all modes approach the fundamental mode of a single 50-nm unit rod, indicated by the dashed line. **b**, When the gaps are increased, all resonance modes tend to merge into one. **c**, The intensities of the first- and third-order modes continuously decrease with increasing gap size, but the intensity of the second-order mode first increases, and then decreases, with a maximum at about 10 nm.

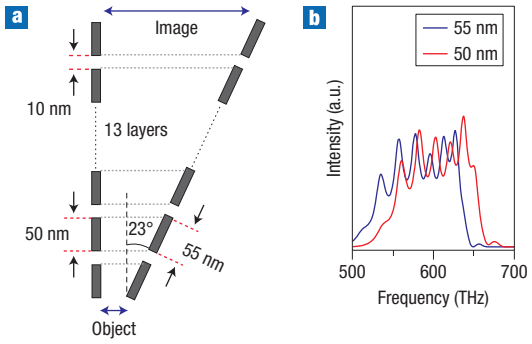

Figure 5 The effect of tapering in stacked layers of metallic nanorods. **a**, When the stacked layers are tapered at a certain angle, it is possible to have a large pixel-to-pixel distance at the image plane, while keeping the subwavelength pixel-to-pixel distance at the object plane constant. This effectively works as the magnification and allows us to record an image of subwavelength resolution using diffraction-limited optics. For a 13-layered arrangement, a tapering angle of 23° is sufficient to obtain image resolution over the diffraction limits. **b**, The resonant band for 13 layers with 50- and 55-nm unit rods, showing an overlap of 90%.

of the latter, with the gap approaching zero. This suggests a strong dependence of the plasmon resonance on the gap size. We therefore examined the gap size dependence of the plasmon resonance for the stacked arrangement. The results for a three-layered arrangement are shown in Fig. 4. When the gap size increases, the first- and third-order modes die out, and the second-order mode achieves the frequency of the fundamental mode of the unit rod, indicated by a dotted line (Fig. 4a). Figure 4b shows the intensity plot of the resonance modes for several values of the gap g, indicating how all modes tend to merge into one when the gap increases. On the one hand, it looks easier to achieve long-distance imaging with a larger gap, because all plasmon energy collects into one mode; however, on the other hand, it is also expected that the plasmon coupling between the rods through the evanescent field will be weaker for larger gaps. It can be seen from the simulation results in Fig. 4c that the intensity of the second-order mode first increases and then decreases with increasing g, and the intensities of the first- and third-order modes continuously decrease and die out quickly. Therefore, optimization of the gap size is very important for efficient coupling, resulting in broad resonance suitable for colour imaging. Figure 4c shows that intensity of the surviving mode has a maximum at the gap size of 10 nm, which gives the optimum value for efficient imaging.

MAGNIFICATION

When one talks about a lens, it is very natural to think about the magnification of the image. For real observation of subwavelength images, it is necessary to magnify the image resolution over the diffraction limit, so that the image can be recorded in the far field, for example, by using a charge-coupled device (CCD) camera. For this purpose, we propose a tapered arrangement of the stacked multilayered nanorod arrays, as suggested in Fig. 1a. For a detailed discussion of the tapering effect, stacked nanorods arranged with a tapering angle are shown in Fig. 5a. The array pitch at the entrance of the nanolens is much smaller than the diffraction limit, which determines the imaging resolution. However, the array pitch at the exit of the nanolens is set to be larger than the diffraction limit, which makes it possible to record the image for real viewing. The magnification is calculated from the ratio of the pitches at the exit and entrance of the nanolens. The tapering angle required for far-field observation of the image depends on the number of layers and is inversely proportional to the number of layers. The imaging mechanism remains exactly the same as discussed in Fig. 2a, except that the pixel-to-pixel distance in the image increases in accordance with the tapering angle. Nanorods oriented at different angles in the tapered arrangement would have different lengths (Fig. 5a), and so would be expected to have different resonance behaviour. However, because of the broad nature of the plasmon resonance, this difference does not drastically affect the colour imaging. For example, if we consider the case of 13-layered arrangement, a tapering angle of 23° would give a diffraction-limited image. As illustrated in Fig. 5a, the length of the unit rod in this case would change from 50 nm to 55 nm. To demonstrate the deviation in resonance behaviour owing to variation in rod lengths, we simulated resonance curves for a 13-layered arrangements with 50- and 55-nm unit rods; the results are shown in Fig. 5b. The resonance band for the 13-layered arrangement with 55-nm unit rods has similar broadening as that with 50-nm unit rods, but it is shifted in position by about 5%. This still gives an overlap of 90% of the resonance bands (Fig. 5b). For an increased number of layers, the required tapering angle would be smaller, resulting in even better overlap. This ensures that a tapered arrangement of a stacked nanorod array would give sufficient magnification for the far-field observation of nanometre-scale objects, keeping the other features intact.

DISCUSSION

The simulation results discussed above confirm that the metallic nanolens proposed here works well for long-distance colour image transfer at subwavelength resolution, with magnification for far-field observation. However, a practical demonstration of the arrangement is limited by achieving accurate growth of the proposed design. Critical challenges in growing the proposed nanolens lie in obtaining uniform nanorod arrays at a tapered angle and in introducing gaps between the arrays. The technique of template-directed electrochemical deposition of silver into a dielectric nanohole array, such as porous alumina, seems to be a potential candidate for the fabrication. It has been shown[11] that successful fabrication of metallic nanowires with nanogaps in the range of five to several hundred nanometres may be achieved using on-wire lithography, which is the same as the technique mentioned above. Others[14] have also demonstrated the growth of nanorods with junctions between the rods defined by monolayers of spacer molecules, which could be another potential technique for growing the proposed nanolens. The challenge, however, still lies in creating uniform gaps in arrays that are tapered. Nevertheless, with current developments in growth technologies, there are indications that carrying out a real experiment based on the proposed scheme for demonstrating subwavelength colour imaging could be possible in the future.

Based on 3D-FDTD simulations, we have proposed a metallic nanolens comprising a stacked arrangement of tapered silver nanorod arrays. We have demonstrated that this nanolens can transfer colour images of nanometre-scale objects over distances of at least micrometre scale with a sufficient amount of magnification for far-field observation. We have also argued that, in principle, the image can be transferred over even longer distance without any significant loss. The proposed nanolens could potentially be a strong imaging tool, for example, for observing individual viruses and other nano-entities in the far field.

METHODS

NUMERICAL SIMULATION

We investigated the imaging features of metallic nanolens by means of numerical simulation using a 3D-FDTD algorithm. Numerical calculations included the Drude dispersion formula, which was applied to the 3D-FDTD algorithm. The frequency dispersion of silver complex permittivity is defined as $\varepsilon_f(\omega) = \varepsilon_\infty - \omega_p^2/(\omega^2 + i\Gamma\omega)$, where ε_∞ is the permittivity at infinity, ω_p is the plasma frequency, and Γ is the damping constant. We set these parameters to closely fit the experimental values[18] for wide range of optical frequencies. The complex permittivity of silver was taken from ref. 18 ($\varepsilon = -9.121 + i0.304$ at $\lambda = 488$ nm) and the values $\varepsilon_\infty = 4.9638$, $\omega_p = 1.4497e + 16$ rad s^{-1} and $\Gamma = 8.33689e + 13$ s^{-1} were obtained from the best fit over the visible range of wavelength ($\lambda \approx 350$–800 nm). For better accuracy in the numerical simulations, the unit cell size in the 3D-FDTD algorithm was chosen to be $1 \times 1 \times 1$ nm^3, and the number of iterations was set to more than 6×10^4 steps to achieve adequate convergence. All results related to the transmission spectra of the rod array shown in this article were obtained by time-domain fast Fourier transform (FFT) of the transmission intensity at the image plane, which was set 10 nm away from the exit of the nanolens and with an impulse oscillation of a dipole source that was set 10 nm away from the entrance of the nanolens.

OPTIMIZATION OF THE NANOLENS PARAMETERS

A rod diameter of 20 nm was selected to obtain a good cylindrical shape in the simulation, with a unit cell size of 1 nm^3. A diameter smaller than 20 nm results in a cross-section that is not a good approximation of a circle, resulting in scattering losses. Accordingly, the length of 50 nm was optimized from the best aspect ratio to resonate the longitudinal mode of the localized surface plasmon at the visible wavelength (in the present case, it was calculated for $\lambda = 488$ nm). The optimum value of pitch for the nanorod array was chosen to be 40 nm, so that crosstalk between the neighbouring nanorods could be avoided[7]. A larger value of pitch leads to costs in terms of resolution, whereas a smaller value costs in terms of blurring of the image. Finally, the gap size was optimized for the best coupling between the nanorods, so that long-distance imaging could be achieved. As shown in Fig. 4c, the highest value of intensity can be achieved at the image plane when gap size g is 10 nm, so this value gives the best coupling for the chosen dimensions of the nanorod array. We finally concluded that unit rods of diameter 20 nm and length 50 nm, arranged at a pitch of 40 nm, give optimized results when these nanorod arrays are arranged with a gap of 10 nm. The optimization was independent of the number of layers in the nanolens.

Received 16 October 2007; accepted 24 April 2008; published 15 June 2008.

References

1. Pendry, J. B. Negative refraction makes a perfect lens. *Phys. Rev. Lett.* **85,** 3966–3969 (2000).
2. Pendry J. B. & Ramakrishna, S. A. Refining the perfect lens. *Physica B* **338,** 329–332 (2003).
3. Smith, D. R. How to build a superlens. *Science* **308,** 502–503 (2005).
4. Shelby, R. A., Smith, D. R. & Schultz, S. Experimental verification of a negative index of refraction. *Science* **292,** 77–79 (2001).
5. Smith, D. R., Pendry, J. B. & Wiltshire, M. C. K. Metamaterials and negative refractive index. *Science* **305,** 788–792 (2004).
6. Fang, N., Lee, H., Sun, C. & Zhang, X. Sub-diffraction-limited optical imaging with a silver superlens. *Science* **308,** 534–537 (2005).
7. Ono, A., Kato, J. & Kawata, S. Subwavelength optical imaging through a metallic nanorod array. *Phys. Rev. Lett.* **95,** 267407 (2005).
8. Kik, P. G., Maier, S. A. & Atwater, H. A. Image resolution of surface-plasmon-mediated near-field focusing with planar metal films in three dimensions using finite-linewidth dipole sources. *Phys. Rev. B* **69,** 045418 (2004).
9. Maier, S. A., Kik, P. G. & Atwater, H. A. Observation of coupled plasmon-polariton modes in Au nanoparticle chain waveguides of different lengths: Estimation of waveguide loss. *Appl. Phys. Lett.* **81,** 1714–1716 (2002).
10. Maier, S. A., Brongersma, M. L., Kik, P. G. & Atwater, H. A. Observation of near-field coupling in metal nanoparticle chains using far-field polarization spectroscopy. *Phys. Rev. B* **65,** 193408 (2002).
11. Qin, L., Park, S., Huang, L. & Mirkin, C. A. On-wire lithography. *Science* **309,** 113–115 (2005).
12. Koenderink, A. F., Hernandez, J. V., Robicheaux, F., Noordam, L. D. & Polman, A. Programmable nanolithography with plasmon nanoparticles arrays. *Nano Lett.* **7,** 745–749 (2007).
13. Srituravanich, W., Fang, N., Sun, C., Luo, Q. & Zhang, X. Plasmonic nanolithography. *Nano Lett.* **4,** 1085–1088 (2004).
14. Aizpurua, J. *et al.* Optical properties of couples metallic nanorods for field-enhanced spectroscopy. *Phys. Rev. B* **71,** 235420 (2005).
15. Liu, Z., Lee, H., Sun, C. & Zhang, X. Far-field optical hyperlens magnifying sub-diffraction-limited object. *Science* **315,** 1686 (2007).
16. Smolyaninov, I. I., Hung, Y. & Davis, C. C. Magnifying superlens in the visible frequency range. *Science* **315,** 1699–1701 (2007).
17. Shvets, G., Trendafilov, S., Pendry, J. B. & Sarychev, A. Guiding, focusing, and sensing on the subwavelength scale using metallic wire arrays. *Phys. Rev. Lett.* **99,** 053903 (2007).
18. Johnson, P. B. & Christy, R. W. Optical constants of nobel metals. *Phys. Rev. B* **6,** 4370–4379 (1972).

Supplementary Information accompanies this paper at www.nature.com/naturephotonics.

Acknowledgements

The authors would like to thank Jun-ichi Kato of RIKEN, Japan, for fruitful discussions. This work was financially supported by the CREST (Core Research for Evolutional Science and Technology) project of JST (Japan Science and Technology Corporation).

Author contributions

All authors collectively conceived the concept of the work presented here. The authors contributed equally in carrying out calculations and in writing this article.

Author information

Reprints and permission information is available online at http://npg.nature.com/reprintsandpermissions/. Correspondence and requests for materials should be addressed to S.K.